Int J Geomath
DOI 10.1007/s13137-012-0041-6

ORIGINAL PAPER

The geomagnetic field gradient tensor

Properties and parametrization in terms of spherical harmonics

Stavros Kotsiaros · Nils Olsen

Received: 3 April 2012 / Accepted: 25 June 2012

Abstract We develop the general mathematical basis for space magnetic gradiometry in spherical coordinates. The magnetic gradient tensor is a second rank tensor consisting of $3 \times 3 = 9$ spatial derivatives. Since the geomagnetic field vector $\mathbf{B}$ is always solenoidal ($\nabla \cdot \mathbf{B} = 0$) there are only eight independent tensor elements. Furthermore, in current free regions the magnetic gradient tensor becomes symmetric, further reducing the number of independent elements to five. In that case $\mathbf{B}$ is a Laplacian potential field and the gradient tensor can be expressed in series of spherical harmonics. We present properties of the magnetic gradient tensor and provide explicit expressions of its elements in terms of spherical harmonics. Finally we discuss the benefit of using gradient measurements for exploring the Earth's magnetic field from space, in particular the advantage of the various tensor elements for a better determination of the small-scale structure of the Earth's lithospheric field.

Keywords Geomagnetic field · Gradient tensor · Space magnetic gradiometry

Mathematics Subject Classification Primary 86A25; Secondary 33C55

1 Introduction

Although an initial global mapping of the Earth's magnetic field intensity has already been performed in the 1960s by the POGO satellite series (Cain 2007), the first global vector mapping of the Earth's magnetic field from space was achieved by the Magsat satellite that flew for 6 months in 1979 and 1980. More recently, the satellites

S. Kotsiaros (✉) · N. Olsen
DTU Space, Technical University of Denmark, Kgs. Lyngby, Denmark
e-mail: skotsiaros@space.dtu.dk

N. Olsen
e-mail: nio@space.dtu.dk

Published online: 24 July 2012

Ørsted (launched in 1999), CHAMP (2000–2010) and SAC-C (2000–2004) provide a continuous mapping and monitoring of the geomagnetic field. In the near future, the *Swarm* satellite mission that is presently under construction by the European Space Agency (ESA) for a scheduled launch in 2012, will provide measurements not only of the magnetic field vector $\mathbf{B}$ but also an estimate of its East–West gradient. This additional parameter contains information especially about North–South oriented features of crustal magnetization, see e.g. Olsen et al. (2004, Fig. 3.5). It is therefore expected that *Swarm* will provide major advances in exploring the geomagnetic field from space.

The derivatives of the magnetic field vector $\mathbf{B}$ in each of the three directions of three-dimensional space define the gradient tensor, consisting of $3 \times 3 = 9$ spatial derivatives and forming a second rank tensor. Each element of the gradient tensor represents a directional filter and thereby emphasizes certain structures of the magnetic field (Schmidt and Clark 2006). The magnetic gradient tensor is therefore a powerful tool for detecting hidden geomagnetic structures by enhancing certain features of the field and suppressing specific undesirable contributions. Due to the similarity of the magnetic and gravity field (under certain conditions) the gravity gradient tensor has similar properties.

Satellite gradiometry and especially its application to gravity field determination has been investigated since the early 1970s. Reed (1973) studied the use of satellite-borne gravity gradient devices for determining the Earth's gravity field. Rummel and Colombo (1985) discuss ways of investigating the gravity field with an orbiting gradiometer measuring the gravity gradient tensor. In 1988 ESA started a series of studies with the goal of preparing the geodetic user community for a dedicated gravity field satellite mission. In the meantime, Rummel et al. (1993) established a comprehensive mathematical basis for satellite gravity gradiometry. In 1999 ESA decided to build and launch the *GOCE* satellite mission which measures the full gravity gradient tensor. *GOCE* was successfully launched in March 2009 and has contributed the most detailed models of Earth's gravity field to date. In the context of inverse problems of mathematical geodesy, Freeden and Nutz (2011) studied the calculation of the gravitational potential at the Earth's surface from the gravity gradient tensor at the height of a low Earth orbiting satellite.

Magnetic gradiometry did not follow the same trend as gravity gradiometry, partly due to the more complicated nature of the geomagnetic field $\mathbf{B}$ which is always solenoidal ($\nabla \cdot \mathbf{B} = 0$), whereas the gravity field $\mathbf{g}$ is always solenoidal and additionally irrotational ($\nabla \times \mathbf{g} = 0$), see Olsen and Kotsiaros (2011). However, magnetic gradiometry has been used for regional studies based on near surface data for decades, see e.g. Pedersen and Rasmussen (1990); Christensen and Rajagopalan (2000); Schmidt and Clark (2000). Some advantages of measuring magnetic field gradients from satellites have been discussed by Harrison and Southam (1991). Purucker et al. (2007) studied the lithospheric field using gradient information constructed from magnetic field measurements collected by the *ST-5* mission that consists of three micro satellites flying in a "string of pearls" constellation. A major step toward magnetic space gradiometry will be undertaken by the *Swarm* satellite mission which provides estimates of the East–West gradient of the vector magnetic field. However, a satellite mission providing global measurements of the full geomagnetic gradient tensor

(i.e. a magnetic mission that is equivalent to what *GOCE* is for the gravity field) has not yet been attempted. Magnetic space gradiometry is a scientifically complicated and technically challenging task, for instance due to the existence of electric currents at satellite altitude.

In this paper we develop a comprehensive mathematical basis for magnetic space-based gradiometry. The properties of the gradient tensor are investigated, and various possible assumptions that simplify its determination are presented. More specifically, we start from the most general case of a solenoid vector field ($\nabla \cdot \mathbf{B} = 0$). This condition reduces the number of independent elements of the gradient tensor from 9 to 8. According to the Mie representation of vector fields (e.g. Backus 1986), every solenoid field—for instance the magnetic field $\mathbf{B}$—can be decomposed into poloidal and toroidal parts. Likewise, the gradient tensor can be constructed separately for the toroidal and poloidal parts of the magnetic field.

Assuming slow time variations (of periods much longer than 1 s) allows one to neglect displacement currents in Maxwell's equations, leading to $\nabla \times \mathbf{B} = \mu_0 \mathbf{J}$ where $\mathbf{J}$ is electrical current density and $\mu_0 = 4\pi 10^{-7}$ Vs/(Am) is the magnetic permeability of free space. In current-free regions ($0 = \mu_0 \mathbf{J} = \nabla \times \mathbf{B}$) the toroidal part of the magnetic field vanishes and the remaining poloidal part may be decomposed into internal and external field parts, an approach termed Gauss' representation. In that case, the magnetic field vector $\mathbf{B} = -\nabla V$ can be derived from a scalar potential V that solves Laplace equation $\nabla^2 V = 0$. Due to $\nabla \times \mathbf{B} = 0$ the magnetic gradient tensor is symmetric which reduces the number of independent elements to 5. Finally, the magnetic gradient tensor can be expanded in terms of Spherical Harmonics (SH) using the same set of Gauss coefficients as for expanding the magnetic scalar potential V. We investigate the information contained in each tensor element and their benefits and limitations for the determination of the Gauss coefficients describing the core and lithospheric parts of the Earth's magnetic field.

The outline of this paper is as follows: In Sect. 2, we present the mathematical basis for space-based magnetic gradiometry and the general expression of the magnetic gradient tensor in Euclidean Space is derived. In Sect. 3, the properties of the gradient tensor are investigated, whereas different assumptions that can simplify the determination of the gradient tensor in space are shown. The gradient tensor is constructed separately for the toroidal and poloidal part of the magnetic field $\mathbf{B}$ in Sect. 4. In Sect. 5 we calculate the magnetic gradient tensor when the magnetic field $\mathbf{B}$ is a Laplacian potential field and in Sect. 6 the magnetic field gradient tensor is parametrized in terms of Spherical Harmonics. The information contained in each tensor element, its benefits and limitations in the determination of the Gauss coefficients are investigated in Sect. 7.

2 The mathematical basis

To derive the magnetic gradient tensor in Euclidean space we define the basis vectors $\mathbf{e}_p$ as

$$\mathbf{e}_p = \frac{\partial \mathbf{r}}{\partial u_p}, \tag{2.1}$$

with $p = 1, 2, 3$. $\mathbf{r}$ is the position vector in one set of coordinates, e.g. in geocentric Cartesian coordinates $\mathbf{r} = (x, y, z)$, whereas $u = (u_1, u_2, u_3)$ is a set of coordinates, e.g. spherical coordinates $u = (r, \theta, \varphi)$. In general the basis vectors $\mathbf{e}_p$ do not have unit magnitude but they may be normalized in order to obtain the unit vectors

$$\hat{\mathbf{e}}_p = \frac{1}{h_p}\frac{\partial \mathbf{r}}{\partial u_p}, \tag{2.2}$$

where the scale factors h_p are given by

$$h_p = \left|\frac{\partial \mathbf{r}}{\partial u_p}\right|. \tag{2.3}$$

Following Talpaert (2002) the gradient of a vector like the magnetic field $\mathbf{B}$ at each point is the tensor field $\nabla\mathbf{B}$ which relates the differential of $\mathbf{B}$ to the position vector elements $\mathrm{d}\mathbf{r}$ such that

$$\mathrm{d}\mathbf{B} = \nabla\mathbf{B}\mathrm{d}\mathbf{r}, \tag{2.4}$$

where the position vector element $\mathrm{d}\mathbf{r}$ is given by

$$\mathrm{d}\mathbf{r} = h_1\mathrm{d}u_1\hat{\mathbf{e}}_1 + h_2\mathrm{d}u_2\hat{\mathbf{e}}_2 + h_3\mathrm{d}u_3\hat{\mathbf{e}}_3 = \begin{pmatrix} h_1\mathrm{d}u_1 \\ h_2\mathrm{d}u_2 \\ h_3\mathrm{d}u_3 \end{pmatrix}, \tag{2.5}$$

(see also Arfken and Weber 2005). Note that the second rank tensor $\nabla\mathbf{B}$ (where ∇ is not an operator and denotes a tensor) should be distinguished from $\boldsymbol{\nabla} \cdot \mathbf{B}$, the divergence of $\mathbf{B}$ (where $\boldsymbol{\nabla}$ is the gradient operator).

Expanding the magnetic field vector $\mathbf{B}$ using the unit vectors defined in Eq. (2.2) yields the column vector $\mathbf{B} = (B_1, B_2, B_3)^{\mathrm{T}}$ (where the superscript T stands for the transpose).

Therefore, the differential $\mathrm{d}\mathbf{B}$ is

$$\begin{aligned}\mathrm{d}\mathbf{B} = {} & \frac{\partial B_1}{\partial u_1}\mathrm{d}u_1\hat{\mathbf{e}}_1 + B_1\frac{\partial \hat{\mathbf{e}}_1}{\partial u_1}\mathrm{d}u_1 + \frac{\partial B_2}{\partial u_1}\mathrm{d}u_1\hat{\mathbf{e}}_2 + B_2\frac{\partial \hat{\mathbf{e}}_2}{\partial u_1}\mathrm{d}u_1 + \frac{\partial B_3}{\partial u_1}\mathrm{d}u_1\hat{\mathbf{e}}_3 \\ & + B_3\frac{\partial \hat{\mathbf{e}}_3}{\partial u_1}\mathrm{d}u_1 + \frac{\partial B_1}{\partial u_2}\mathrm{d}u_2\hat{\mathbf{e}}_1 + B_1\frac{\partial \hat{\mathbf{e}}_1}{\partial u_2}\mathrm{d}u_2 + \frac{\partial B_2}{\partial u_2}\mathrm{d}u_2\hat{\mathbf{e}}_2 + B_2\frac{\partial \hat{\mathbf{e}}_2}{\partial u_2}\mathrm{d}u_2 \\ & + \frac{\partial B_3}{\partial u_2}\mathrm{d}u_2\hat{\mathbf{e}}_3 + B_3\frac{\partial \hat{\mathbf{e}}_3}{\partial u_2}\mathrm{d}u_2 + \frac{\partial B_1}{\partial u_3}\mathrm{d}u_3\hat{\mathbf{e}}_1 + B_1\frac{\partial \hat{\mathbf{e}}_1}{\partial u_3}\mathrm{d}u_3 + \frac{\partial B_2}{\partial u_3}\mathrm{d}u_3\hat{\mathbf{e}}_2 \\ & + B_2\frac{\partial \hat{\mathbf{e}}_2}{\partial u_3}\mathrm{d}u_3 + \frac{\partial B_3}{\partial u_3}\mathrm{d}u_3\hat{\mathbf{e}}_3 + B_3\frac{\partial \hat{\mathbf{e}}_3}{\partial u_3}\mathrm{d}u_3.\end{aligned} \tag{2.6}$$

Using the position vector element, Eq. (2.5), then $\mathrm{d}\mathbf{B} = \nabla\mathbf{B}\mathrm{d}\mathbf{r}$, Eq. (2.4), can be expressed with the help of Eq. (2.6) and the magnetic field gradient tensor $\nabla\mathbf{B}$ can be therefore expressed as

$$\nabla\mathbf{B} = \begin{pmatrix} \frac{1}{h_1}\left(\frac{\partial B_1}{\partial u_1} + \sum_{p=1}^{3} B_p \frac{\partial \hat{\mathbf{e}}_p}{\partial u_1}\hat{\mathbf{e}}_1\right) \frac{1}{h_2}\left(\frac{\partial B_1}{\partial u_2} + \sum_{p=1}^{3} B_p \frac{\partial \hat{\mathbf{e}}_p}{\partial u_2}\hat{\mathbf{e}}_1\right) \\ \frac{1}{h_1}\left(\frac{\partial B_2}{\partial u_1} + \sum_{p=1}^{3} B_p \frac{\partial \hat{\mathbf{e}}_p}{\partial u_1}\hat{\mathbf{e}}_2\right) \frac{1}{h_2}\left(\frac{\partial B_2}{\partial u_2} + \sum_{p=1}^{3} B_p \frac{\partial \hat{\mathbf{e}}_p}{\partial u_2}\hat{\mathbf{e}}_2\right) \cdots \\ \frac{1}{h_1}\left(\frac{\partial B_3}{\partial u_1} + \sum_{p=1}^{3} B_p \frac{\partial \hat{\mathbf{e}}_p}{\partial u_1}\hat{\mathbf{e}}_3\right) \frac{1}{h_2}\left(\frac{\partial B_3}{\partial u_2} + \sum_{p=1}^{3} B_p \frac{\partial \hat{\mathbf{e}}_p}{\partial u_2}\hat{\mathbf{e}}_3\right) \end{pmatrix}$$
$$\begin{pmatrix} \frac{1}{h_3}\left(\frac{\partial B_1}{\partial u_3} + \sum_{p=1}^{3} B_p \frac{\partial \hat{\mathbf{e}}_p}{\partial u_3}\hat{\mathbf{e}}_1\right) \\ \cdots \frac{1}{h_3}\left(\frac{\partial B_2}{\partial u_3} + \sum_{p=1}^{3} B_p \frac{\partial \hat{\mathbf{e}}_p}{\partial u_3}\hat{\mathbf{e}}_2\right) \\ \frac{1}{h_3}\left(\frac{\partial B_3}{\partial u_3} + \sum_{p=1}^{3} B_p \frac{\partial \hat{\mathbf{e}}_p}{\partial u_3}\hat{\mathbf{e}}_3\right) \end{pmatrix}. \tag{2.7}$$

A more compact form for its elements is

$$[\nabla\mathbf{B}]_{ij} = \frac{1}{h_j}\left(\frac{\partial B_i}{\partial u_j} + \sum_{p=1}^{3} B_p \frac{\partial \hat{\mathbf{e}}_p}{\partial u_j}\hat{\mathbf{e}}_i\right), \tag{2.8}$$

with $i, j = 1, 2, 3$, whereas from Eq. (2.2) we have

$$\frac{\partial \hat{\mathbf{e}}_p}{\partial u_j} = -\frac{1}{h_p^2}\frac{\partial h_p}{\partial u_j}\frac{\partial \mathbf{r}}{\partial u_p} + \frac{1}{h_p}\frac{\partial^2 \mathbf{r}}{\partial u_j \partial u_p}. \tag{2.9}$$

In the case of spherical coordinates $u = (r, \theta, \varphi)$ the scale factors h_p are

$$h_1 = 1, \tag{2.10a}$$
$$h_2 = r, \tag{2.10b}$$
$$h_3 = r\sin\theta, \tag{2.10c}$$

and the position vector $\mathbf{r}$ and the position vector element $d\mathbf{r}$ are

$$\mathbf{r} = \begin{pmatrix} r\sin\theta\cos\varphi \\ r\sin\theta\sin\varphi \\ r\cos\theta \end{pmatrix} \tag{2.11}$$

$$d\mathbf{r} = \begin{pmatrix} dr \\ rd\theta \\ r\sin\theta d\varphi \end{pmatrix} \tag{2.12}$$

(Arfken and Weber 2005). Therefore, making use of Eqs. (2.9) and (2.8), the magnetic gradient tensor $\nabla\mathbf{B}$ in spherical coordinates is given by

$$\nabla \mathbf{B} = \begin{pmatrix} \frac{\partial B_r}{\partial r} & \frac{1}{r}\frac{\partial B_r}{\partial \theta} - \frac{1}{r}B_\theta & \frac{1}{r\sin\theta}\frac{\partial B_r}{\partial \varphi} - \frac{1}{r}B_\varphi \\ \frac{\partial B_\theta}{\partial r} & \frac{1}{r}\frac{\partial B_\theta}{\partial \theta} + \frac{1}{r}B_r & \frac{1}{r\sin\theta}\frac{\partial B_\theta}{\partial \varphi} - \frac{\cot\theta}{r}B_\varphi \\ \frac{\partial B_\varphi}{\partial r} & \frac{1}{r}\frac{\partial B_\varphi}{\partial \theta} & \frac{1}{r\sin\theta}\frac{\partial B_\varphi}{\partial \varphi} + \frac{1}{r}B_r + \frac{\cot\theta}{r}B_\theta \end{pmatrix}. \tag{2.13}$$

3 Properties of magnetic field gradient tensor

Full characterization of the magnetic field gradient tensor, Eq. (2.13), requires the specification of nine independent elements. However, making use of Gauss' law of magnetism,

$$\nabla \cdot \mathbf{B} = 0, \tag{3.1}$$

reduces the number of independent elements from 9 to 8. Physically, Eq. (3.1) means that magnetic monopoles (in analogy to electric charges) do not exist. In spherical coordinates Eq. (3.1) reads

$$0 = \nabla \cdot \mathbf{B} = \frac{1}{r^2}\frac{\partial}{\partial r}(r^2 B_r) + \frac{1}{r\sin\theta}\frac{\partial}{\partial \theta}(\sin\theta B_\theta) + \frac{1}{r\sin\theta}\frac{\partial B_\varphi}{\partial \varphi} \tag{3.2}$$

$$= \frac{\partial B_r}{\partial r} + \frac{2}{r}B_r + \frac{1}{r}\frac{\partial B_\theta}{\partial \theta} + \frac{\cot\theta}{r}B_\theta + \frac{1}{r\sin\theta}\frac{\partial B_\varphi}{\partial \varphi}. \tag{3.3}$$

Comparison with Eq. (2.13) shows that the divergence of the vector corresponds to the trace of the gradient tensor, which is always zero because $\nabla \cdot \mathbf{B} = 0$:

$$\nabla \cdot \mathbf{B} = tr(\nabla \mathbf{B}) = 0. \tag{3.4}$$

A powerful aspect of the gradient tensor can be recognized by starting from Ampere's law in the quasi-static approximation

$$\nabla \times \mathbf{B} = \mu_0 \mathbf{J} \tag{3.5}$$

which, as mentioned before, holds for processes with time-scales longer than 1 s, a condition that is very well satisfied in geomagnetism. In spherical coordinates the curl of $\mathbf{B}$ is

$$\begin{aligned} \mu_0 \mathbf{J} = \nabla \times \mathbf{B} = &\left(\frac{1}{r}\frac{\partial B_\varphi}{\partial \theta} + \frac{\cot\theta}{r}B_\varphi - \frac{1}{r\sin\theta}\frac{\partial B_\theta}{\partial \varphi}\right)\hat{\mathbf{e}}_r \\ &+ \left(\frac{1}{r\sin\theta}\frac{\partial B_r}{\partial \varphi} - \frac{\partial B_\varphi}{\partial r} - \frac{1}{r}B_\varphi\right)\hat{\mathbf{e}}_\theta \\ &+ \left(\frac{\partial B_\theta}{\partial r} + \frac{1}{r}B_\theta - \frac{1}{r}\frac{\partial B_r}{\partial \theta}\right)\hat{\mathbf{e}}_\varphi. \end{aligned} \tag{3.6}$$

The difference of the gradient tensor with its transpose yields

$$\nabla\mathbf{B}-\nabla\mathbf{B}^T=\begin{pmatrix} 0 & \frac{1}{r}\frac{\partial B_r}{\partial\theta}-\frac{1}{r}B_\theta-\frac{\partial B_\theta}{\partial r} & \cdots \\ \frac{\partial B_\theta}{\partial r}-\frac{1}{r}\frac{\partial B_r}{\partial\theta}+\frac{1}{r}B_\theta & 0 & \cdots \\ \frac{\partial B_\varphi}{\partial r}-\frac{1}{r\sin\theta}\frac{\partial B_r}{\partial\varphi}+\frac{1}{r}B_\varphi & \frac{1}{r}\frac{\partial B_\varphi}{\partial\theta}-\frac{1}{r\sin\theta}\frac{\partial B_\theta}{\partial\varphi}+\frac{\cos\theta}{r\sin\theta}B_\varphi & \cdots \\ & & \end{pmatrix}\begin{matrix} \frac{1}{r\sin\theta}\frac{\partial B_r}{\partial\varphi}-\frac{1}{r}B_\varphi-\frac{\partial B_\varphi}{\partial r} \\ \frac{1}{r\sin\theta}\frac{\partial B_\theta}{\partial\varphi}-\frac{\cos\theta}{r\sin\theta}B_\varphi-\frac{1}{r}\frac{\partial B_\varphi}{\partial\theta} \\ 0 \end{matrix} \tag{3.7}$$

and with $\mathbf{J}=J_r\hat{\mathbf{e}}_r+J_\theta\hat{\mathbf{e}}_\theta+J_\varphi\hat{\mathbf{e}}_\varphi$ Eqs. (3.5) and (3.7) can be combined to

$$\nabla\mathbf{B}-\nabla\mathbf{B}^T=\mu_0\begin{pmatrix} 0 & -J_\varphi & +J_\theta \\ +J_\varphi & 0 & -J_r \\ -J_\theta & +J_r & 0 \end{pmatrix}. \tag{3.8}$$

The gradient tensor therefore provides information on the in-situ electrical current density $\mathbf{J}=(J_r,J_\theta,J_\varphi)^T$. An important aspect of Eq. (3.8) is that $\nabla\mathbf{B}=\nabla\mathbf{B}^T$ in current free regions ($\mathbf{J}=0$), which results in a symmetric gradient tensor. This reduces the number of independent elements to 5 which significantly simplifies the determination of the gradient tensor.

The general expression of the gradient tensor in spherical coordinates, Eq. (2.13), indicates that all tensor elements except those in the first column contain, in addition to the field derivatives along the direction θ or φ, contributions from the field components B_r, B_θ, B_φ. Thus, they represent a mixture of contributions from the field and its spatial derivatives. However, when studying small-scale variations, e.g. the lithospheric field, it is possible to simplify the gradient tensor. Since the geomagnetic field is dominated by the large-scale main field (i.e. contributions described by spherical harmonic degrees up to, say, $n=13$) the terms of the gradient tensor that include the field (rather than its spatial derivative) can be neglected, as shown e.g. by Olsen and Kotsiaros (2011). In that case Eq. (2.13) reduces to

$$\nabla\mathbf{B}\approx\begin{pmatrix} \frac{\partial B_r}{\partial r} & \frac{1}{r}\frac{\partial B_r}{\partial\theta} & \frac{1}{r\sin\theta}\frac{\partial B_r}{\partial\varphi} \\ \frac{\partial B_\theta}{\partial r} & \frac{1}{r}\frac{\partial B_\theta}{\partial\theta} & \frac{1}{r\sin\theta}\frac{\partial B_\theta}{\partial\varphi} \\ \frac{\partial B_\varphi}{\partial r} & \frac{1}{r}\frac{\partial B_\varphi}{\partial\theta} & \frac{1}{r\sin\theta}\frac{\partial B_\varphi}{\partial\varphi} \end{pmatrix} \tag{3.9}$$

and the tensor elements contain only contributions from the field derivatives along each direction but not from the vector field $\mathbf{B}$ itself.

4 Toroidal–poloidal decomposition

According to the Mie representation, a solenoid vector like the magnetic vector $\mathbf{B}$ can be written uniquely as the sum of a toroidal and a poloidal part (cf. Mie 1908; Backus 1986; Backus et al. 1996; Sabaka et al. 2010). Each part is derived via curl operations:

$$\mathbf{B} = \mathbf{B}_{\text{tor}} + \mathbf{B}_{\text{pol}} \tag{4.1}$$

$$\mathbf{B} = \nabla \times \mathbf{r}\Phi + \nabla \times \nabla \times \mathbf{r}\Psi \tag{4.2}$$

where Φ and Ψ are the toroidal and poloidal scalar potentials, respectively. In spherical coordinates this decomposition is given by

$$\mathbf{B} = \underbrace{\begin{pmatrix} 0 \\ \frac{1}{\sin\theta}\frac{\partial}{\partial\varphi}\Phi \\ -\frac{\partial}{\partial\theta}\Phi \end{pmatrix}}_{\text{toroidal part}} + \underbrace{\begin{pmatrix} -\Delta_s(r\Psi) \\ \frac{1}{r}\frac{\partial}{\partial\theta}(r\Psi)' \\ \frac{1}{r\sin\theta}\frac{\partial}{\partial\varphi}(r\Psi)' \end{pmatrix}}_{\text{poloidal part}} \tag{4.3}$$

with $(r\Psi)' = \frac{d(r\Psi)}{dr}$ and $\Delta_s = \frac{1}{r^2\sin\theta}\frac{\partial}{\partial\theta}\left(\sin\theta\frac{\partial}{\partial\theta}\right) + \frac{1}{r^2\sin^2\theta}\frac{\partial^2}{\partial\varphi^2}$ is the horizontal part of the Laplacian. An expansion of the scalar potentials Φ and Ψ in a series of spherical harmonics is given in Olsen (1997).

The gradient tensor of the toroidal, resp. poloidal, part follows as

$$\nabla\mathbf{B}_{\text{tor}} = \begin{pmatrix} 0 & -\frac{1}{r\sin\theta}\frac{\partial\Phi}{\partial\varphi} & \frac{1}{r}\frac{\partial\Phi}{\partial\theta} \\ \frac{1}{\sin\theta}\frac{\partial^2\Phi}{\partial r\partial\varphi} & \frac{\partial}{r\partial\theta}\left(\frac{1}{\sin\theta}\frac{\partial\Phi}{\partial\varphi}\right) & \frac{\cos\theta}{r\sin\theta}\frac{\partial\Phi}{\partial\theta} + \frac{1}{r\sin^2\theta}\frac{\partial^2\Phi}{\partial\varphi^2} \\ -\frac{\partial^2\Phi}{\partial r\partial\theta} & -\frac{1}{r}\frac{\partial^2\Phi}{\partial\theta^2} & -\frac{\partial}{r\partial\theta}\left(\frac{1}{\sin\theta}\frac{\partial\Phi}{\partial\varphi}\right) \end{pmatrix} \tag{4.4}$$

$$\nabla\mathbf{B}_{\text{pol}} = \begin{pmatrix} -\frac{\partial}{\partial r}\Delta_s(r\Psi) & -\frac{1}{r}\frac{\partial}{\partial\theta}\left(\Delta_s(r\Psi) + \frac{1}{r}(r\Psi)'\right) & \cdots \\ \frac{\partial}{\partial r}\left(\frac{\partial(r\Psi)'}{r\partial\theta}\right) & -\frac{1}{r}\Delta_s(r\Psi) + \frac{1}{r^2}\frac{\partial^2}{\partial\theta^2}(r\Psi)' & \cdots \\ \frac{1}{\sin\theta}\frac{\partial}{\partial r}\left(\frac{\partial(r\Psi)'}{r\partial\varphi}\right) & \frac{\partial}{\partial\theta}\left(\frac{1}{r^2\sin\theta}\frac{\partial(r\Psi)'}{\partial\varphi}\right) & \cdots \end{pmatrix}$$

$$\begin{pmatrix} -\frac{1}{r\sin\theta}\frac{\partial}{\partial\varphi}\left(\Delta_s(r\Psi) + \frac{1}{r}(r\Psi)'\right) \\ \cdots \\ \frac{\partial}{\partial\theta}\left(\frac{1}{r^2\sin\theta}\frac{\partial(r\Psi)'}{\partial\varphi}\right) \\ -\frac{1}{r}\Delta_s(r\Psi) + \frac{1}{r^2\sin\theta}\left(\frac{1}{\sin\theta}\frac{\partial^2}{\partial\varphi^2} + \cos\theta\frac{\partial}{\partial\theta}\right)(r\Psi)' \end{pmatrix}. \tag{4.5}$$

The general condition that the trace of the gradient tensor is zero, Eq. (3.4), holds also for the gradient tensor of the toroidal and poloidal parts separately.

5 Laplacian potential approximation

In case of vanishing currents ($\mathbf{J} = 0$) in a shell where the magnetic measurements are taken, i.e. a source-free region, the toroidal field $\mathbf{B}_{\text{tor}}$ vanishes and the poloidal field $\mathbf{B}_{\text{pol}}$ can be decomposed into a part $\mathbf{B}_{\text{i}}$ caused by currents inside the shell and another part $\mathbf{B}_{\text{e}}$ caused by currents outside the shell (cf. Backus et al. 1996, chap. 5):

$$\mathbf{B} = \mathbf{B}_{\text{i}} + \mathbf{B}_{\text{e}}. \tag{5.1}$$

Since the magnetic vector $\mathbf{B}$ within the shell is curl-free,

$$\mu_0 \mathbf{J} = \nabla \times \mathbf{B} = 0, \tag{5.2}$$

it can be written as the (negative) gradient of a scalar potential V,

$$\mathbf{B} = -\nabla V \tag{5.3}$$

and because of $\nabla \cdot \mathbf{B} = 0$ the potential V has to obey Laplace's equation: $\nabla^2 V = 0$. Similar to Eq. (5.1), the scalar potential V can be split into an internal part V_{i} and an external part V_{e}

$$V = V_{\text{i}} + V_{\text{e}}, \tag{5.4}$$

each of which may be expanded in series of spherical harmonics, as discussed in the next section. The magnetic field vector $\mathbf{B}$ follows as

$$\mathbf{B} = \underbrace{\begin{pmatrix} -\dfrac{\partial V_{\text{i}}}{\partial r} \\ -\dfrac{1}{r}\dfrac{\partial V_{\text{i}}}{\partial \theta} \\ -\dfrac{1}{r \sin\theta}\dfrac{\partial V_{\text{i}}}{\partial \varphi} \end{pmatrix}}_{\mathbf{B}_{\text{i}}} + \underbrace{\begin{pmatrix} -\dfrac{\partial V_{\text{e}}}{\partial r} \\ -\dfrac{1}{r}\dfrac{\partial V_{\text{e}}}{\partial \theta} \\ -\dfrac{1}{r \sin\theta}\dfrac{\partial V_{\text{e}}}{\partial \varphi} \end{pmatrix}}_{\mathbf{B}_{\text{e}}}. \tag{5.5}$$

According to Eq. (2.13) the gradient tensor is then given by

$$\nabla \mathbf{B} = \begin{pmatrix} -\dfrac{\partial^2 V}{\partial r^2} & -\dfrac{\partial}{\partial r}\left(\dfrac{1}{r}\dfrac{\partial V}{\partial \theta}\right) & \cdots \\ -\dfrac{\partial}{\partial r}\left(\dfrac{1}{r}\dfrac{\partial V}{\partial \theta}\right) & -\dfrac{1}{r}\dfrac{\partial V}{\partial r} - \dfrac{1}{r^2}\dfrac{\partial^2 V}{\partial \theta^2} & \cdots \\ -\dfrac{\partial}{\partial r}\left(\dfrac{1}{r \sin\theta}\dfrac{\partial V}{\partial \varphi}\right) & -\dfrac{\partial}{\partial \theta}\left(\dfrac{1}{r^2 \sin\theta}\dfrac{\partial V}{\partial \varphi}\right) & \\ -\dfrac{\partial}{\partial r}\left(\dfrac{1}{r \sin\theta}\dfrac{\partial V}{\partial \varphi}\right) & & \\ \cdots -\dfrac{\partial}{\partial \theta}\left(\dfrac{1}{r^2 \sin\theta}\dfrac{\partial V}{\partial \varphi}\right) & & \\ -\dfrac{1}{r}\dfrac{\partial V}{\partial r} - \dfrac{\cot\theta}{r^2}\dfrac{\partial V}{\partial \theta} - \dfrac{1}{r^2 \sin^2\theta}\dfrac{\partial^2 V}{\partial \varphi^2} & & \end{pmatrix}, \tag{5.6}$$

where $V = V_\mathrm{i} + V_\mathrm{e}$. Equation (5.6) can be written independently for the internal part V_i and the external part V_e, respectively. The trace of this tensor is equal to $-\nabla^2 V$ which is zero, as expected. Additionally, the gradient tensor is symmetric, which is consistent with what was stated in Sect. 3. Hence only five tensor elements have to be specified in order to fully determine the magnetic gradient tensor.

6 The spherical harmonic representation

The scalar potential V can be expanded in series of spherical harmonics:

$$V = \mathbb{R}\left\{ a \sum_{n=1}^{N} \sum_{m=0}^{n} \gamma_n^m \exp(im\varphi) \left(\frac{a}{r}\right)^{n+1} P_n^m(\cos\theta) + a \sum_{n=1}^{N_\mathrm{e}} \sum_{m=0}^{n} \delta_n^m \exp(im\varphi) \left(\frac{r}{a}\right)^{n} P_n^m(\cos\theta) \right\}, \tag{6.1}$$

where $\mathbb{R}\{\cdots\}$ denotes the real part of the series and i is the imaginary number, a is a reference radius (typically Earth's mean radius $a = 6{,}371.2$ km is chosen), $P_n^m(\cos\theta)$ are the associated Schmidt semi-normalized Legendre functions of degree n and order m, $\gamma_n^m = g_n^m - ih_n^m$ and $\delta_n^m = q_n^m - is_n^m$ are the complex Gauss coefficients describing sources internal and external to the Earth, respectively. Theoretically, the series extends up to infinite degree, but since in practice there is only a limited number of measurements at discrete points, the series are truncated at some largest degree N and N_e, respectively.

The magnetic field vector follows as

$$\mathbf{B}_\mathrm{i} = \mathbb{R}\left\{ \begin{pmatrix} \sum_{n=1}^{N} \sum_{m=0}^{n} (n+1)\gamma_n^m \exp(im\varphi) \left(\frac{a}{r}\right)^{(n+2)} P_n^m(\cos\theta) \\ -\sum_{n=1}^{N} \sum_{m=0}^{n} \gamma_n^m \exp(im\varphi) \left(\frac{a}{r}\right)^{(n+2)} \frac{dP_n^m(\cos\theta)}{d\theta} \\ -\sum_{n=1}^{N} \sum_{m=0}^{n} \frac{m}{\sin\theta} i\gamma_n^m \exp(im\varphi) \left(\frac{a}{r}\right)^{(n+2)} P_n^m(\cos\theta) \end{pmatrix} \right\}, \tag{6.2a}$$

$$\mathbf{B}_\mathrm{e} = \mathbb{R}\left\{ \begin{pmatrix} -\sum_{n=1}^{N_\mathrm{e}} \sum_{m=0}^{n} n\delta_n^m \exp(im\varphi) \left(\frac{r}{a}\right)^{(n-1)} P_n^m(\cos\theta) \\ -\sum_{n=1}^{N_\mathrm{e}} \sum_{m=0}^{n} \delta_n^m \exp(im\varphi) \left(\frac{r}{a}\right)^{(n-1)} \frac{dP_n^m(\cos\theta)}{d\theta} \\ -\sum_{n=1}^{N_\mathrm{e}} \sum_{m=0}^{n} \frac{m}{\sin\theta} i\delta_n^m \exp(im\varphi) \left(\frac{r}{a}\right)^{(n-1)} P_n^m(\cos\theta) \end{pmatrix} \right\}. \tag{6.2b}$$

Given Eq. (2.13), the gradient tensor elements of the internal part $[\nabla \mathbf{B}_\mathrm{i}]_{jk}$ and external part $[\nabla \mathbf{B}_\mathrm{e}]_{jk}$ of the magnetic field can be expanded in series of spherical harmonics. Here the first subscript, j, stands for the vector component for which the derivative is taken, while the second, k, indicates the direction of the spatial derivative,

with $j, k = r, \theta, \varphi$. Since we are dealing with the potential case (i.e. absence of electrical currents), the tensor is symmetric and therefore only six out of nine elements are presented.

$$[\nabla \mathbf{B}_{\mathrm{i}}]_{jk} = \mathbb{R}\left\{\frac{1}{a}\sum_{n=1}^{N}\sum_{m=0}^{n}\gamma_n^m \exp(im\varphi)\left(\frac{a}{r}\right)^{(n+3)} P_{n,\,jk}^{m,\,\mathrm{i}}(\cos\theta)\right\} \tag{6.3}$$

with:

$$P_{n,\,rr}^{m,\,\mathrm{i}}(\cos\theta) = -(n+1)(n+2)P_n^m(\cos\theta) \tag{6.4a}$$

$$P_{n,\,\theta\theta}^{m,\,\mathrm{i}}(\cos\theta) = (n+1)P_n^m(\cos\theta) - \frac{d^2 P_n^m(\cos\theta)}{d\theta^2} \tag{6.4b}$$

$$P_{n,\,\varphi\varphi}^{m,\,\mathrm{i}}(\cos\theta) = \left[\frac{m^2}{\sin^2\theta} + (n+1)\right] P_n^m(\cos\theta) - \cot\theta \frac{d P_n^m(\cos\theta)}{d\theta} \tag{6.4c}$$

$$P_{n,\,r\theta}^{m,\,\mathrm{i}}(\cos\theta) = (n+2)\frac{d P_n^m(\cos\theta)}{d\theta} \tag{6.4d}$$

$$P_{n,\,r\varphi}^{m,\,\mathrm{i}}(\cos\theta) = \frac{m(n+2)}{\sin\theta} i P_n^m(\cos\theta) \tag{6.4e}$$

$$P_{n,\,\theta\varphi}^{m,\,\mathrm{i}}(\cos\theta) = \frac{m\cos\theta}{\sin^2\theta} i P_n^m(\cos\theta) - \frac{m}{\sin\theta} i \frac{d P_n^m(\cos\theta)}{d\theta} \tag{6.4f}$$

and

$$[\nabla \mathbf{B}_{\mathrm{e}}]_{jk} = \mathbb{R}\left\{\frac{1}{a}\sum_{n=1}^{N_{\mathrm{e}}}\sum_{m=0}^{n}\delta_n^m \exp(im\varphi)\left(\frac{r}{a}\right)^{(n-2)} P_{n,\,jk}^{m,\,\mathrm{e}}(\cos\theta)\right\} \tag{6.5}$$

with

$$P_{n,\,rr}^{m,\,\mathrm{e}}(\cos\theta) = -n(n-1)P_n^m(\cos\theta) \tag{6.6a}$$

$$P_{n,\,\theta\theta}^{m,\,\mathrm{e}}(\cos\theta) = -n P_n^m(\cos\theta) - \frac{d^2 P_n^m(\cos\theta)}{d\theta^2} \tag{6.6b}$$

$$P_{n,\,\varphi\varphi}^{m,\,\mathrm{e}}(\cos\theta) = \left[\frac{m^2}{\sin^2\theta} - n\right] P_n^m(\cos\theta) - \cot\theta \frac{d P_n^m(\cos\theta)}{d\theta} \tag{6.6c}$$

$$P_{n,\,r\theta}^{m,\,\mathrm{e}}(\cos\theta) = -(n-1)\frac{d P_n^m(\cos\theta)}{d\theta} \tag{6.6d}$$

$$P_{n,\,r\varphi}^{m,\,\mathrm{e}}(\cos\theta) = -\frac{m(n-1)}{\sin\theta} i P_n^m(\cos\theta) \tag{6.6e}$$

$$P_{n,\,\theta\varphi}^{m,\,\mathrm{e}}(\cos\theta) = \frac{m\cos\theta}{\sin^2\theta} i P_n^m(\cos\theta) - \frac{m}{\sin\theta} i \frac{d P_n^m(\cos\theta)}{d\theta}. \tag{6.6f}$$

As mentioned earlier, the trace of the magnetic gradient tensor is always zero and therefore $P^{m,\,\mathrm{i}}_{n,\,rr} + P^{m,\,\mathrm{i}}_{n,\,\theta\theta} + P^{m,\,\mathrm{i}}_{n,\,\varphi\varphi} = 0$ and similarly $P^{m,\,\mathrm{e}}_{n,\,rr} + P^{m,\,\mathrm{e}}_{n,\,\theta\theta} + P^{m,\,\mathrm{e}}_{n,\,\varphi\varphi} = 0$.

7 The gradient tensor as a tool for magnetic field determination

After having introduced in the previous sections a mathematical representation of the magnetic gradient tensor, we now discuss the problem of using magnetic gradient observations to explore the geomagnetic field.

The goal of geomagnetic field modelling is to estimate, from geomagnetic field observations, the spherical harmonic expansion coefficients (g_n^m, h_n^m) and (q_n^m, s_n^m) of Eq. (6.1) describing sources of internal, resp. external, origin. These observations can be the components of the magnetic vector $\mathbf{B}$, the magnetic field intensity $|\mathbf{B}|$ and/or elements of the gradient tensor. In this section we investigate geomagnetic field modelling using the various elements of the magnetic gradient tensor. For this task we will only consider a determination of the Gauss coefficients (g_n^m, h_n^m) of internal origin. In addition, we concentrate on a determination of the small-scale lithospheric field.

Determination of Gauss coefficients from observations of the magnetic field vector or the gradient tensor elements is a linear problem, and therefore the model vector $\mathbf{m}$ containing the unknown Gauss coefficients (the model parameters (g_n^m, h_n^m)) is related to the data vector $\mathbf{d}$ (containing observations of the vector component or gradient tensor elements) as

$$\mathbf{d} = \mathbf{G}\mathbf{m} \tag{7.1}$$

where $\mathbf{G}$ is the data kernel matrix. An estimate $\hat{\mathbf{m}}$ of the model vector $\mathbf{m}$ in the (weighted) Least-Square sense results in

$$\hat{\mathbf{m}} = (\mathbf{G}^T\mathbf{C}_d^{-1}\mathbf{G})^{-1}\mathbf{G}^T\mathbf{C}_d^{-1}\mathbf{d} \tag{7.2}$$

$$= (\mathbf{G}^T\mathbf{G})^{-1}\mathbf{G}^T\mathbf{d}, \tag{7.3}$$

where $\mathbf{C}_d$ is the data covariance matrix which is assumed to be diagonal with elements σ_d^2, corresponding to independent observations with common variance σ_d^2. The diagonal elements of the model covariance matrix

$$\mathbf{C}_m = \sigma_d^2(\mathbf{G}^T\mathbf{G})^{-1} \tag{7.4}$$

are the variances σ_g^2 of the estimated model parameters, i.e. of the Gauss coefficients (g_n^m, h_n^m). $\mathbf{C}_m$ is independent of the data vector $\mathbf{d}$, i.e. of the actual magnetic data, but depends on the satellite positions and on the type of observation, i.e. which vector components or gradient tensor elements are considered in the inversion process. Therefore, given a satellite orbit configuration and a certain type of observations, maps of the variances σ_g^2 give information on the performance of the magnetic field determination for that given orbit and observation type.

Approximate analytic expressions for the covariance matrix $\mathbf{C}_m$ and thereby for the variances σ_g^2 of the estimated model parameters have been derived by Lowes (1966)

and Langel (1987) for the case that the observations consist of N_d measurements of all three components (B_r, B_θ, B_φ) of the magnetic vector equally distributed by area on the sphere (or weighted by $\sin\theta$ if they are taken by a polar orbiting satellite and equally spaced in time).[1] In that case $\mathbf{G}^T\mathbf{G}$, and hence also $\mathbf{C}_m$, approach (in the limiting case of an infinite number of observations) diagonal matrices due to the orthogonality of spherical harmonics, and the variances of the Gauss coefficients are given by

$$\sigma_g^2 \approx \sigma_d^2 \left(\frac{r}{a}\right)^{2n+4} \frac{1}{N_d(n+1)}, \quad \text{if } \mathbf{d} = \{B_r, B_\theta, B_\varphi\} \tag{7.5}$$

(cf. Eq. 124 of Langel 1987). Note that these variances do not depend on the order m of the spherical harmonics, i.e. they are equal for all Gauss coefficients of a given degree n. If only measurements of the radial vector component B_r are used the corresponding variances of the Gauss coefficients are

$$\sigma_g^2 \approx \sigma_d^2 \left(\frac{r}{a}\right)^{2n+4} \frac{2n+1}{N_d(n+1)^2}, \quad \text{if } \mathbf{d} = \{B_r\} \tag{7.6}$$

which is larger than Eq. (7.5) by a factor between 3/2 (for $n = 1$) and 2 (for $n \to \infty$).

Analytic expressions for σ_g^2 do not exist if the data consist of the horizontal field components B_θ or B_φ since in those cases $\mathbf{G}^T\mathbf{G}$ is not a diagonal matrix and it is not possible to analytically derive its inverse. In order to study these cases we therefore rely on numerical simulations, similar to the ones performed in Olsen et al. (2010). For those we used synthetic data from a satellite in a polar circular orbit at 400 km altitude. They span a period of one month with a sampling rate of 30 s, which gives us $N_d = 89{,}280$ magnetic measurements in total. Since the data are equally spaced in time we applied weights $w = \sin\theta$ in order to simulate an equal area distribution. The diagonal elements, σ_g^2, of the numerically computed model covariance matrix $\mathbf{C}_m$ are shown in Fig. 1 in dependence on degree n and order m (where $m \geq 0$ belongs to the coefficients g_n^m while $m < 0$ belongs to h_n^m). The left part of the figure represents the variances for the case that observations of B_r are used; this map corresponds to the analytic expression for σ_g^2 given in Eq. (7.6). The other parts of the figure show the variances σ_g^2 for the cases that observations consist of the magnetic field components B_θ (middle) or B_φ (right). Note that σ_g^2 in these cases depend on both degree n and order m. Overall, the maps show the information contained in each vector component. White represents low information content, whereas green represents high information content.

If the data consist of the radial gradient of the radial vector component, $[\nabla\mathbf{B}]_{rr}$, a similar analytic approach as in the case of B_r as data can be used to derive the variances

[1] There is a typo in the right-hand side of equation 122a and 122c of Langel (1987) which correctly should read $\delta_{k,j}[n(n+1)/(2n+1) - m/2]$ and $\delta_{k,j}[(n+1)^2/(2n+1)]$, respectively.

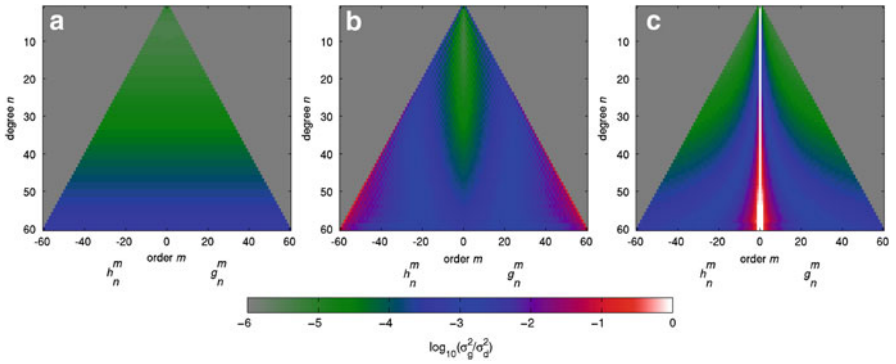

Fig. 1 Variance of the estimated internal Gauss coefficients from 89,280 data points of each field component, **a** B_r, **b** B_θ and **c** B_φ, obtained by a polar orbiting satellite at 400 km altitude. *White* represents low information content, whereas *green* represents high information content (colour figure online)

of the Gauss coefficients. In that case $\mathbf{G}^T\mathbf{G}$ can be approximated by

$$\begin{aligned}\mathbf{G}^T\mathbf{G} &\approx \frac{N_d}{4\pi a^2}\int_0^{2\pi}\int_0^{\pi}\left\{\begin{matrix}\cos(m\varphi)\cos(m'\varphi)\\ \sin(m\varphi)\sin(m'\varphi)\end{matrix}\right\}[(n+1)(n+2)][(n'+1)(n'+2)]\\ &\quad\times\left(\frac{a}{r}\right)^{(n+3)}\left(\frac{a}{r}\right)^{(n'+3)}P_n^m(\cos\theta)P_{n'}^{m'}(\cos\theta)\sin\theta\,\mathrm{d}\theta\mathrm{d}\varphi\\ &= \frac{1}{a^2}\left(\frac{a}{r}\right)^{(2n+6)}\frac{N_d[(n+1)(n+2)]^2}{2n+1}\delta_{m,m'}\delta_{n,n'}\end{aligned}\tag{7.7}$$

due to the orthogonality of the spherical harmonics. The variances of the Gauss coefficients follow as

$$\sigma_g^2 \approx (a\sigma_d)^2\left(\frac{r}{a}\right)^{(2n+6)}\frac{2n+1}{N_d[(n+1)(n+2)]^2},\quad \text{if } \mathbf{d}=\{[\nabla\mathbf{B}]_{rr}\}.\tag{7.8}$$

In this case the relative variance of the estimated Gauss coefficients, σ_g, is again independent of the order m. Note that the variance of the observations, σ_d, has the units $\frac{\mathrm{nT}}{\mathrm{km}}$, since it refers to gradient observations, in contrast to the variance σ_d in Eqs. (7.5) and (7.6) where it has the units nT, since it refers to vector observations.

For large n the variances of the Gauss coefficients obtained from vector data, cf. Eq. (7.6), is proportional to $1/n$ while those obtained using gradient data, cf. Eq. (7.8) behaves like $1/n^3$. This indicates the advantage of gradient information for determination of the small-scale (i.e. high-degree) structure of the lithospheric field.

No analytic formula exist for the cases when the data consist of the other tensor elements since they depend on a more complex combination of Legendre functions, see Eqs. (6.4b), (6.4c) and (6.4f), and orthogonality cannot be assumed. We therefore have to rely on numerical simulations similar to the ones presented in Fig. 1.

Maps of the obtained variances σ_d^2 are presented in Fig. 2 for the various type of magnetic gradient observations. Figure 2a corresponds to the element $[\nabla\mathbf{B}]_{rr}$

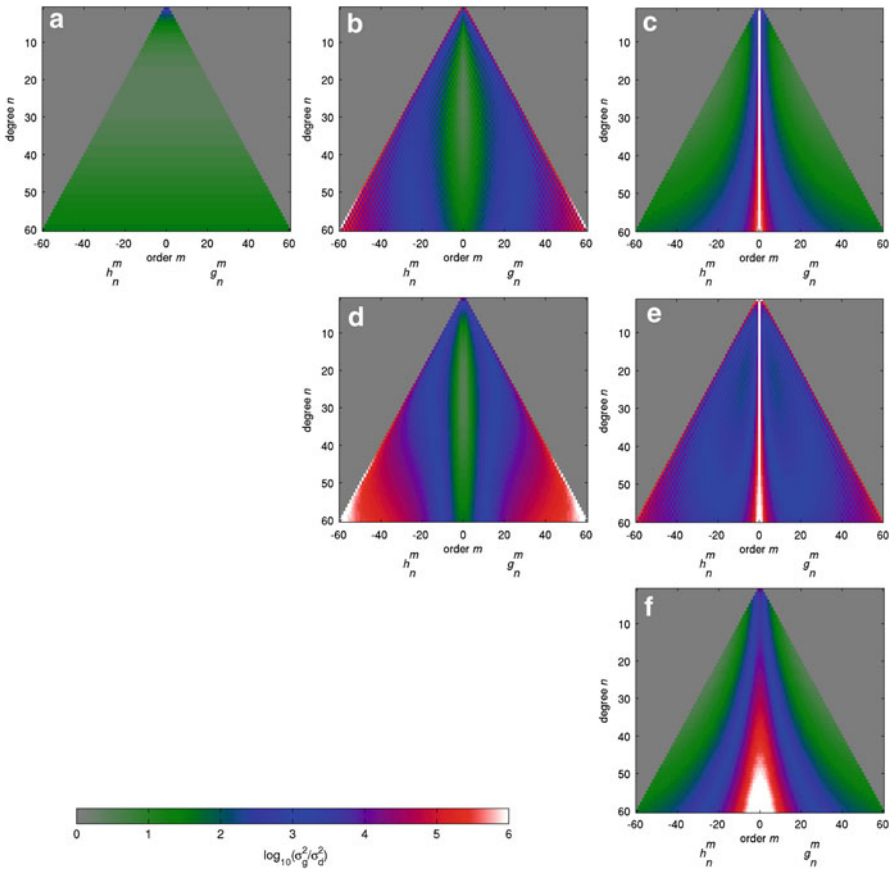

Fig. 2 Variance of the estimated internal Gauss coefficients from 89,280 data points of each tensor element, **a** $[\nabla\mathbf{B}]_{rr}$, **b** $[\nabla\mathbf{B}]_{r\theta}$, **c** $[\nabla\mathbf{B}]_{r\varphi}$, **d** $[\nabla\mathbf{B}]_{\theta\theta}$, **e** $[\nabla\mathbf{B}]_{\theta\varphi}$, **f** $[\nabla\mathbf{B}]_{\varphi\varphi}$, obtained by a polar orbiting satellite at 400 km altitude. *White* represents low information content, whereas *green* represents high information content (colour figure online)

(i.e. the Gauss coefficients are estimated by measurements of $[\nabla\mathbf{B}]_{rr}$ only) and shows the advantage of knowing the radial gradient of the radial magnetic field component B_r; the analytic expression of these variances is given by Eq. (7.8). Figure 2b corresponds to the element $[\nabla\mathbf{B}]_{r\theta}$ and shows the advantage of knowing the North–South gradient of the radial magnetic field component B_r. Figure 2c corresponds to the element $[\nabla\mathbf{B}]_{r\varphi}$ and shows the benefit of having measurements of the East–West gradient of the radial field component B_r. Figure 2d, e illustrate the benefit of measuring the North–South, resp. East–West, gradient of the co-latitudinal field component B_θ. At last, Fig. 2f shows the advantage of having measurements of the East–West gradient of the longitudinal field component B_φ. Note that due to the symmetry of the magnetic gradient tensor in current-free regions the information contained in $[\nabla\mathbf{B}]_{r\varphi}$ is identical to that contained in $[\nabla\mathbf{B}]_{\varphi r}$. Likewise, $[\nabla\mathbf{B}]_{\varphi\theta}$ and $[\nabla\mathbf{B}]_{\theta\varphi}$ contain the same information, and also $[\nabla\mathbf{B}]_{\theta r}$ and $[\nabla\mathbf{B}]_{r\theta}$. The lower left triangle part of Fig. 2 is therefore identical to its upper right part.

Variances obtained from $[\nabla \mathbf{B}]_{rr}$, the radial gradient of the radial field component, cf. Fig. 2a, are independent of the order m and resolve best the higher degrees n. There is a focus on higher degrees which is imposed by the factor $\left(\frac{r}{a}\right)^{(2n+6)}$ and therefore is characteristic of the orbit height. On the other hand, the relative variance σ_g^2/σ_d^2 of the Gauss coefficients estimated by the North–South gradients of B_r, cf. Fig. 2b, depends also on the order m. In particular, there is a degradation toward high-order coefficients. In case of the East–West gradient of B_r, cf. Fig. 2c, there is an improved estimation of the sectoral ($n = m$) and near-sectoral ($n \approx m$) coefficients. This also shows that relying on the East–West gradient of the radial field component alone does not allow the determination of the zonal terms ($m = 0$). This issue can however be solved by including other types of data, such as vector components or other tensor elements, in addition to the East–West gradient.

Knowledge of the North–South gradient of the co-latitudinal field component B_θ improves the estimation of the low-order coefficients, see Fig. 2d. Information on the East–West gradient of B_θ, i.e. Fig. 2e, improves the estimation of the tesseral coefficients. However, the same issue as in Fig. 2c appears, which is that East–West gradient data alone do not allow the zonal terms ($m = 0$) to be determined. Finally, information on the East–West gradient of the longitudinal field component B_φ improves the estimation of the high-order coefficients, see Fig. 2f. Unlike the other two cases, zonal terms can now also be determined with this particular East–West gradient tensor element (although the quality is degraded especially for the high degree values). The reason is that, unlike the other two cases, the East–West gradient of the longitudinal field component $[\nabla \mathbf{B}]_{\varphi\varphi}$ does not only depend on terms that are sensitive to the order m (such as B_φ, or $\frac{\partial B_\theta}{\partial \varphi}$), but also on the term $\frac{1}{r} B_r$, which is sensitive only to the degree n, see Eq. (2.13). Therefore, the determination of zonal terms, which was not possible by the other East–West gradients, can be achieved from $[\nabla \mathbf{B}]_{\varphi\varphi}$.

In general, Fig. 2 shows that each tensor element improves the determination of coefficients of certain degrees n and orders m. The information provided by each tensor element, and thus the particular benefits in the determination of certain coefficients, can be combined and thereby a more precise determination of the complete Gauss coefficients set can be achieved. The optimal combination of tensor element observations depends, however, on several factors, such as orbit configuration, attitude and instrument errors along certain directions.

At high latitudes the disturbance magnetic field (i.e. due to magnetospheric and ionospheric currents) is much stronger and more complex compared to low and middle latitudes, mainly because of the occurrence of field-aligned currents. Therefore, present estimates of the high-latitude anomaly fields (e.g. lithospheric field) are not fully reliable since they might be contaminated by external current contributions. Measurements of the individual gradient tensor elements yield information on the in situ electrical current density, as indicated by Eq. (3.8). Consequently, the impact of the field-aligned currents on each tensor element can be determined and hence, accordingly combining (or even down-weighting and excluding) these tensor elements in the determination of the lithospheric field has the potential of obtaining more reliable estimates of the lithospheric field at high latitudes.

8 Conclusions

The *Swarm* satellite mission will provide a new dimension of geomagnetic exploration from space by measuring, in addition to the magnetic field vector, also an estimate of the East–West gradient of the geomagnetic field. This contains valuable information on North–South oriented features of crustal magnetization. However, a similar resolution of East–West oriented structures is not possible with *Swarm* since this requires measurement of the North–South magnetic field gradient. Going beyond *Swarm's* limitations, a possible future way for exploring the Earth's magnetic field from space would be to move towards a full gradiometry mission.

In this paper we have developed a comprehensive mathematical basis for magnetic space gradiometry. The magnetic gradient tensor $\nabla\mathbf{B}$ is a second rank tensor consisting of $3 \times 3 = 9$ spatial derivatives. Making use of the general constraint that the magnetic field is always solenoidal ($\boldsymbol{\nabla} \cdot \mathbf{B} = 0$) reduces the number of independent tensor elements from 9 to 8. Furthermore, in a current free region ($\mathbf{J} = 0$) the magnetic gradient tensor becomes symmetric, further reducing the number of independent elements to 5. In that case the magnetic field $\mathbf{B}$ is a Laplacian potential field and the gradient tensor can be used to estimate the spherical harmonic expansion coefficients (Gauss coefficients) of the magnetic potential.

The possible benefit of using gradient tensor measurements is exploited by looking at the variances of the estimated model parameters (i.e. the Gauss coefficients). For ideally sampled data, the variances depend only on the satellite orbit and the type of field observations (e.g. which tensor elements are measured). Maps of the variances of the estimated Gauss coefficients show the performance of the magnetic field determination for a given orbit and observation type. Each tensor element provides particular information and improves the estimation of Gauss coefficients of specific degree and order. Therefore, the combination of individual tensor elements for specific ranges of degree and order has the potential for improving the overall determination of the Gauss coefficients and hence for obtaining a more accurate description of the geomagnetic field. Present determinations of the high-latitude lithospheric fields are for example not fully reliable mainly due to the existence of field aligned currents. However, the magnetic gradient tensor provides information on the in situ electrical current density. Therefore, the impact of field aligned currents on each tensor element can be determined, and hence these elements can be suitably combined to obtain more accurate estimates of the high-latitude lithospheric field.

In order to investigate the information content (i.e. the variances of the Gauss coefficients) in each vector component as well as in each gradient tensor element, we perform a simulation based on synthetic data generated on a polar circular orbit using a basic input model. That input model provides the static magnetic field contribution from the core and lithosphere. A full end-to-end mission simulation based on a more sophisticated orbit and on a more realistic input model, which also accounts for the highly time dependent magnetic field contributions due to currents in the ionosphere and magnetosphere, is the topic of a forthcoming paper.

References

Arfken, G.B., Weber, H.J.: Mathematical Methods for Physicists, 6th edn. Elsevier Academic Press, Amsterdam (2005)

Backus, G.: Poloidal and toroidal fields in geomagnetic field modeling. Rev. Geophys. **24**, 75–109 (1986)

Backus, G., Parker, R., Constable, C.: Foundations of Geomagnetism. Cambridge University Press, Cambridge (1996)

Cain, J.C.: POGO (OGO-2, -4 and -6 spacecraft). In: Gubbins, D., Herrero-Bervera, E. (eds.) Encyclopedia of Geomagnetism and Paleomagnetism, pp. 828–829, Springer, Heidelberg (2007)

Christensen, A., Rajagopalan, S.: The magnetic vector and gradient tensor in mineral and oil exploration. Preview **84**, 77 (2000)

Freeden, W., Nutz, H.: Satellite gravity gradiometry as tensorial inverse problem. GEM Int. J. Geomath. **2**, 177–218 (2011)

Harrison, C., Southam, J.: Magnetic field gradients and their uses in the study of the Earth's magnetic field. J. Geomagn. Geoelectr. **43**, 585–599 (1991)

Langel, R.A.: The main field. In: Jacobs, J.A. (ed) Geomagnetism, vol. 1, pp. 249–512. Academic Press, London (1987)

Lowes, F.J.: Mean-square values on sphere of spherical harmonic vector fields. J. Geophys. Res. **71**, 2179 (1966)

Mie, G.: Considerations on the optic of turbid media, especially colloidal metal sols. Ann. Phys. **25**, 377–442 (1908)

Olsen, N.: Ionospheric *F* region currents at middle and low latitudes estimated from Magsat data. J. Geophys. Res. **102**(A3), 4563–4576 (1997)

Olsen, N., Kotsiaros, S.: Magnetic satellite missions and data. In: Mandea, M., Korte, M. (eds.) Geomagnetic Observations and Models, IAGA Special Sopron Book Series, Chap. 2, vol. 5, pp. 27–44. Springer, Heidelberg. doi:10.1007/978-90-481-9858-0_2 (2011)

Olsen, N., Friis-Christensen, E., Hulot, G., Korte, M., Kuvshinov, A.V., Lesur, V., Lühr, H., Macmillan, S., Mandea, M., Maus, S., Purucker, M., Reigber, C., Ritter, P., Rother, M., Sabaka, T., Tarits, P., Thomson, A.: *Swarm*: End-to-End Mission Performance Simulator Study, ESA Contract No 17263/03/NL/CB. DSRI Report 1/2004, Danish Space Research Institute, Copenhagen (2004)

Olsen, N., Hulot, G., Sabaka, T.J.: Measuring the Earth's magnetic field from space: concepts of past, present and future missions. Space Sci. Rev. **155**, 65–93. doi:10.1007/s11214-010-9676-5 (2010)

Pedersen, L.B., Rasmussen, T.M.: The gradient tensor of potential field anomalies: Some implications on data collection and data processing of maps. Geophysics **55**(12), 1558–1566 (1990)

Purucker, M., Sabaka, T., Le, G., Slavin, J.A., Strangeway, R.J., Busby, C.: Magnetic field gradients from the st-5 constellation: improving magnetic and thermal models of the lithosphere. Geophys. Res. Lett. **34**(24), L24,306 (2007)

Reed, G.B.: Application of kinematical geodesy for determining the short wave length components of the gravity field by satellite gradiometry. Reports of the Department of Geodetic Science (Report No. 201) (1973)

Rummel, R., Colombo, O.: Gravity field determination from satellite gradiometry. J. Geodesy **59**, 233–246 (1985)

Rummel, R., van Gelderen, M., Koop, R., Schrama, E., Sanso, F., Brovelli, M., Miggliaccio, F., Sacerdote, F.: Spherical harmonic analysis of satellite gradiometry. Technical Report (1993)

Sabaka, T.J., Hulot, G., Olsen, N.: Mathematical properties relevant to geomagnetic field modelling. In: Freeden, W., Nashed, Z., Sonar, T. (eds.) Handbook of Geomathematics. Springer, Heidelberg (2010)

Schmidt, P., Clark, D.: Advantages of measuring the magnetic gradient tensor. Preview **85**, 26–30 (2000)

Schmidt, P., Clark, D.: The magnetic gradient tensor: its properties and uses in source characterization. Lead. Edge **25**(1), 75–78 (2006)

Talpaert, Y.: Tensor analysis and continuum mechanics. Kluwer Academic Publishers, Dordrecht (2002)